2022

Serum Protein Signatures Using Aptamer-Based Proteomics for Minimal Change Disease and Membranous Nephropathy

Daniel A. Muruve

Hanna Debiec

Simon T. Dillon

Xuesong Gu

Emmanuelle Plaisier

See next page for additional authors

Authors

Daniel A. Muruve, Hanna Debiec, Simon T. Dillon, Xuesong Gu, Emmanuelle Plaisier, Handan Can, Hasan H. Otu, Towia A. Libermann, and Pierre Ronco

KI REPORTS
KIReports.org
CLINICAL RESEARCH

Serum Protein Signatures Using Aptamer-Based Proteomics for Minimal Change Disease and Membranous Nephropathy

Daniel A. Muruve[1,7], Hanna Debiec[2,7], Simon T. Dillon[3], Xuesong Gu[3], Emmanuelle Plaisier[2,4], Handan Can[5], Hasan H. Otu[5], Towia A. Libermann[3,8] and Pierre Ronco[2,6,8]

[1]Department of Medicine, Snyder Institute for Chronic Diseases, University of Calgary, Calgary, Alberta, Canada; [2]Unité Mixte de Recherche S1155, Sorbonne Université and Institut National de la Santé et de la Recherche Médicale, Paris, France; [3]Department of Medicine, BIDMC Genomics, Proteomics, Bioinformatics, and Systems Biology Center and Dana Farber/Harvard Cancer Center—Cancer Proteomics Core, Division of Interdisciplinary Medicine and Biotechnology, Beth Israel Deaconess Medical Center and Harvard Medical School, Boston, Massachusetts, USA; [4]Department of Nephrology, Association pour l'Utilisation du Rein Artificiel Paris Plaisance, Paris, France; [5]Department of Electrical and Computer Engineering, University of Nebraska—Lincoln, Lincoln, Nebraska, USA; and [6]Department of Nephrology, Center Hospitalier du Mans, Le Mans, France

Introduction: Minimal change disease (MCD) and membranous nephropathy (MN) are glomerular diseases (glomerulonephritis [GN]) that present with the nephrotic syndrome. Although circulating PLA2R antibodies have been validated as a biomarker for MN, the diagnosis of MCD and PLA2R-negative MN still relies on the results of kidney biopsy or empirical corticosteroids in children. We aimed to identify serum protein biomarker signatures associated with MCD and MN pathogenesis using aptamer-based proteomics.

Methods: Quantitative SOMAscan proteomics was applied to the serum of adult patients with MCD ($n = 15$) and MN ($n = 37$) and healthy controls ($n = 20$). Associations between the 1305 proteins detected with SOMAscan were assessed using multiple statistical tests, expression pattern analysis, and systems biology analysis.

Results: A total of 208 and 244 proteins were identified that differentiated MCD and MN, respectively, with high statistical significance from the healthy controls (Benjamin-Hochberg [BH] $P < 0.0001$). There were 157 proteins that discriminated MN from MCD (BH $P < 0.05$). In MCD, 65 proteins were differentially expressed as compared with MN and healthy controls. When compared with MCD and healthy controls, 44 discriminatory proteins were specifically linked to MN. Systems biology analysis of these signatures identified cell death and inflammation as key pathways differentiating MN from MCD and healthy controls. Dysregulation of fatty acid metabolism pathways was confirmed in both MN and MCD as compared with the healthy subjects.

Conclusion: SOMAscan represents a promising proteomic platform for biomarker development in GN. Validation of a greater number of discovery biomarkers in larger patient cohorts is needed before these data can be translated for clinical care.

Kidney Int Rep (2022) **7,** 1539–1556; https://doi.org/10.1016/j.ekir.2022.04.006
KEYWORDS: minimal change disease; membranous nephropathy; proteomics; systems biology

See Commentary on Page 1450

GN comprise a broad family of rare kidney diseases that are associated with significant morbidity and high health care costs.[1] Owing to their rarity, the molecular and genetic understanding of GN has lagged other disciplines, hampering the development of advanced diagnostic technologies, targeted therapies, and precision medicine for these conditions. Although a few serologic tests for GN exist, they are largely insufficient to address the complex clinical needs of patients and physicians.[2]

MCD and MN are immune GNs of unknown etiology in children and adults (incidence of approximately 2

Correspondence: Pierre Ronco, Institut National de la Santé et de la Recherche Médicale (INSERM) UMRS 1155, Hôpital Tenon, Rue de la Chine 4, 75020 Paris, France. E-mail: pierreronco@yahoo.fr; or Towia Libermann, Research North Building, Room 380C, Beth Israel Deaconess Medical Center, 99 Brookline Avenue, Boston, Massachusetts 02115, USA. E-mail: tliberma@bidmc.harvard.edu

[7]DAM and HD contributed equally and are considered as co-first authors.

[8]TAL and PR contributed equally and are considered as co-senior authors.

Received 22 January 2022; revised 30 March 2022; accepted 4 April 2022; published online 14 April 2022

per 100,000).[1] Both MCD and MN present with the nephrotic syndrome and are often indistinguishable on clinical grounds. With the exception of MN, the clinical diagnosis and approach for the nephrotic syndrome have not changed significantly in >50 years and rely on an invasive kidney biopsy which is associated with a 6% to 7% risk of major bleeding complications.[3] In children, the nephrotic syndrome is generally first treated with an empirical course of corticosteroids. A blood test or biomarker that identifies steroid-responsive MCD would reduce the frequency of kidney biopsies in adults and guide appropriate corticosteroid therapy in children with the nephrotic syndrome. This is significant because corticosteroid dose reduction and personalized corticosteroid-sparing therapies are the top patient-reported priorities for the nephrotic syndrome and MCD in children.[4] In MN, at least 30% of patients will undergo spontaneous remission and require no disease-modifying therapies, whereas the remaining 70% of patients are at risk of developing progressive chronic kidney disease.[2] Although antibodies to PLA2R and THSD7A are clinically accurate diagnostic biomarkers of primary autoimmune disease that have improved the diagnosis and management of MN, they only capture approximately 75% and <5% of patients, respectively.[2] Furthermore, PLA2R and THSD7A antibodies at baseline and in follow-up only modestly predict spontaneous remission and do not reliably correlate with long-term outcomes, and many patient outliers exist.[5–7] Thus, decision-making and management of patients with MN remain somewhat empirical, driven by clinical judgment, serial serologic/conventional diagnostic testing, and follow-up.

Given that GNs have distinct pathogenic mechanisms and require different therapies, noninvasive molecular diagnosis should be feasible to refine medical decision-making and patient care. For example, blood biomarkers that improve risk stratification of MN at the time of diagnosis would permit earlier and tailored initiation of immunosuppression regimens and avoid inappropriate treatment in patients who may experience a spontaneous remission. Furthermore, the discovery of additional biomarkers as surrogates of disease activity would improve patient assessment and address the significant lag between serologic and clinical remission (i.e., proteinuria).

Discovery proteomics for GNs to date has been hampered by the interference created by abundant proteins, such as albumin or immunoglobulins, present in patient blood and urine biospecimens which prevent the identification of low-abundance proteins that may be highly clinically relevant. The objective of this study was to characterize the serum protein profiles of MCD and MN using the SOMAscan proteomics platform to begin to address some of the clinical issues related to these disorders. SOMAscan is a highly multiplexed, sensitive, and quantitative immune-like proteomic tool for biomarker discovery. SOMAscan uses high-affinity, protein capture-modified DNA aptamers, which are oligonucleotides that bind with high specificity and high affinity to preselected proteins.[8,9] SOMAscan quantifies >1300 and more recently up to 7000 clinically relevant proteins and transforms each individual protein concentration into a corresponding SOMAmer concentration, which is then quantified using a DNA microarray readout.[8,9] SOMAscan has been applied successfully to large clinical biomarker discovery studies,[9] including diabetic kidney disease and dialysis-dependent acute kidney injury,[10–12] strongly supporting its potential to discover kidney disease biomarkers. Key advantages of SOMAscan are a median lower limit of detection of 40 fM (<1 pg/ml), an unprecedented dynamic range of >10 logs, and outstanding reproducibility (median coefficient of variation <5%). SOMAscan's depth of coverage offers exceptional power for biomarker discovery with a greater dynamic range than most other proteomic technologies. SOMAscan is particularly well suited for studying GN because it provides a more complete picture of the complex biological pathways that drive disease pathogenesis. Using this technology, we identified unique serum molecular profiles that clearly distinguished healthy controls, MCD, and MN. In particular, proteins in the inflammation/immune, coagulation, and cell death pathways were differentially regulated in MCD and MN, setting the stage for the development of noninvasive diagnostic biomarkers for these common causes of the nephrotic syndrome.

METHODS

Patient Cohort and Biospecimens

Sera were obtained from 52 randomly selected male and female patients presenting to Hôpital Tenon, Paris, France, with MCD ($n = 15$) and MN ($n = 37$) between 2005 and 2016 (MCD) and 1999 and 2012 (MN). Patient characteristics were collected at the time of enrollment and retrieved from the patient medical record. Patient clinical characteristics are presented in Figure 1. There were 32 patients with MN positive for PLA2R antibodies, 1 for anti-THSD7A, and 5 were double negative. MN antibodies were not tested in 1 patient. Serum was isolated from blood collection tubes and stored at −80° C. All patient sera were drawn at the time of biopsy, and none had received immunosuppressive therapy before biospecimen collection. All patients

Table 1. Differentially regulated proteins in MN versus MCD and N

Gene symbol	Fold change (MCD/N)	BH *P* value	Fold change (MN/N)	BH *P* value	Fold change (MN/MCD)	BH *P* value
Downregulated proteins between MN vs. MCD and N						
CASP3	1.14	0.456954	−1.64	0.000002	−1.86	0.000237
POR	1.18	0.896748	−1.83	0.000002	−2.18	0.001885
CBX5	1.06	0.245514	−1.14	0.006435	−1.22	0.003026
TOP1	1.17	0.394072	−1.33	0.000374	−1.55	0.006046
KPNB1	1.87	0.275356	−1.56	0.000678	−2.92	0.00631
XRCC6	1.18	0.180195	−1.24	0.008284	−1.46	0.008574
CD47	1.06	0.223886	−1.10	0.025378	−1.16	0.009332
YWHAB;YWHAE;YWHAG;YWHAH; YWHAQ;YWHAZ;SFN	1.11	0.206434	−1.21	0.003534	−1.35	0.009332
CHEK1	1.01	0.7663	−1.14	0.009395	−1.15	0.01166
CRYZL1	1.29	0.252001	−1.27	0.003282	−1.64	0.011783
IGF1	1.02	0.919997	−1.21	0.000453	−1.23	0.014591
NME2	1.46	0.593527	−3.08	0.000001	−4.50	0.014744
LYN	1.24	0.611296	−1.41	0.000967	−1.75	0.015513
YWHAZ	1.17	0.575513	−1.35	0.004933	−1.57	0.020487
SNX4	−1.06	0.231136	−1.90	0	−1.80	0.021726
FOLH1	−1.02	0.894164	−1.29	0.001248	−1.26	0.027259
CSNK2A1 CSNK2B	1.07	0.998697	−1.41	0.000479	−1.51	0.03089
IL1B	−1.32	0.078033	−1.82	0.000002	−1.38	0.030892
ALDOA	2.10	0.558837	−1.51	0.001345	−3.17	0.034084
SRC	1.18	0.805007	−1.36	0.001804	−1.61	0.039331
ENTPD3	1.05	0.196096	−1.09	0.040597	−1.15	0.041261
XPNPEP1	1.11	0.949155	−1.39	0.000206	−1.54	0.043322
EGF	1.16	0.439583	−1.26	0.028881	−1.47	0.046149
CST7	−1.25	0.081315	−1.73	0	−1.39	0.046149
Upregulated proteins between MN vs. MCD and N						
F2	−1.28	0.060437	1.52	0.001063	1.94	0.000255
MAP2K4	1.16	0.998929	2.22	0	1.91	0.001464
RBP4	1.05	0.797639	1.53	0.000003	1.45	0.002167
PDCD1LG2	−1.17	0.056333	1.23	0.012721	1.44	0.002393
IL1RL1	−1.14	0.684203	1.55	0.003282	1.77	0.006046
HRG	−1.08	0.749027	1.50	0.000272	1.51	0.006661
IL17RC	−1.07	0.109203	1.33	0.010651	1.43	0.007021
MAPK11	1.08	0.973743	1.59	0.000007	1.46	0.007172
TFPI	1.23	0.222482	1.81	0	1.48	0.009332
CST3	1.16	0.339782	1.92	0.000008	1.66	0.01302
SPOCK2	−1.08	0.318686	1.28	0.005903	1.37	0.013999
HAMP	1.82	0.275356	4.22	0.000006	2.31	0.014591
PI3	1.24	0.460855	2.39	0.000034	1.93	0.017006
TFF2	1.06	0.634787	1.49	0.000342	1.41	0.028657
MED1	1.06	0.397784	1.40	0.000375	1.32	0.03089
PSMA2	1.69	0.260856	3.09	0.00001	1.82	0.032104
ANG	1.17	0.405444	1.60	0.000015	1.37	0.035229
LGALS3	1.03	0.782452	1.29	0.000949	1.25	0.039025
CCL11	1.02	0.880309	1.36	0.001669	1.32	0.042719
REG4	1.06	0.607167	1.61	0.000815	1.52	0.042719

BH, Benjamin-Hochberg; MN, membranous nephropathy; MCD, minimal change disease; N, healthy controls.

provided informed consent to allow the use of their medical information and biospecimens for kidney disease research. Serum samples from adult healthy controls ($n = 20$, 13 males, 7 females, mean age 41.2 years) were obtained from the Etablissement Français du Sang in Lyon, France. Healthy donors are screened for past medical history, including surgery, transfusions, long-term taken medications, recent occurrences (tattoo, piercing, small surgery, infection), recent travels, sexual practices, and laboratory tests such as HIV and hepatitis serology.

The study was approved by an institutional review board in Paris, France (Comité de Protection des Personnes, Ile-de-France XI). The registry of kidney biopsies and the related biobank at Tenon Hospital was authorized by the Commission nationale de

l'informatique et des libertés. Serum was stored in the Center de Ressources Biologiques, located at Tenon Hospital (statement no. DC-2009-965; label "TUMO0616," by INCa and DGOS). Identification and storage of samples were performed according to standard operating procedures. We used previously collected samples, and the secondary use was authorized by the primary owner. The collection has been declared at Institut National de la Santé et de la Recherche Médicale.

SOMAscan Proteomics

SOMAscan proteomics analysis using serum samples was performed at the BIDMC Genomics, Proteomics, Bioinformatics and Systems Biology Center (Boston, MA). A 50 µl of patient serum was processed on the SOMAscan assay 1.3k for human serum, which measures the expression of 1305 human proteins using highly selective, single-stranded, modified Slow Off-rate Modified DNA Aptamers and analyzed according to standard protocols for biological fluids from SomaLogic that have been described elsewhere.[8,13–17] In brief, fluorescence-labeled SOMAscan aptamers for the 1305 proteins, coupled with a photocleavable linker and biotin, were immobilized on beads and divided into 3 dilution bins (0.05%, 1%, 40%) corresponding to the abundance of their target proteins in serum. Then, the serum test samples, diluted to the 3 bin concentrations, were incubated with the corresponding highly specific SOMAmer-bead panel. Unbound proteins were removed by washing, and SOMAmer-bound proteins were biotinylated followed by photocleavage to remove the beads. The SOMAmer-protein complexes from the 3 different bins were then combined and captured on streptavidin beads. After washing, fluorescently labeled SOMAscan aptamers were eluted using a denaturing buffer and hybridized to an Agilent microarray containing the complementary strand oligonucleotide to each SOMAmer for a microarray readout as a proxy for the protein concentration which reports the data as relative fluorescence units as a surrogate of protein expression levels. Furthermore, 5 pooled human serum controls and 1 no-protein buffer control were run in parallel with the serum test samples per run of 24 test samples. Owing to the tight coefficient of variation of approximately 5%, the samples are run as singlets. Sample-to-sample variability was further controlled by several hybridization spike-in controls.

Data quality control, signal calibration, hybridization control normalization to remove individual sample variance, median signal and normalization to remove intersample plate differences, and calibration for interplate differences based on the pooled serum samples included on each plate were done according to the manufacturer's protocol to correct for technical and batch effects in data introduced during the sample processing. All samples passed the SomaLogic standard quality control and normalization criteria for the manual 1.3k assay.

Biostatistics and Systems Biology Analysis

Differential protein expression was assessed using t test with BH correction for multiple hypothesis testing.[18,19] Sample clustering was performed using hierarchical clustering and principal component analysis (PCA).[20] To acquire new insights into potential pathophysiological pathways and biological functions underlying the MN-related and MCD-related serum protein signatures and to more precisely understand the complex interactions between the differentially expressed proteins and candidate upstream regulators, we performed functional category, canonical pathway, interactive network, upstream regulator, and regulator effect analyses of the dysregulated proteins for each comparator group using the Ingenuity Pathway Analysis (IPA) software tool (QIAGEN, Redwood City, CA),[21] a repository of biological interactions and functions created from millions of individually modeled relationships ranging from the molecular (proteins, genes) to organism (diseases) level.

Predictive models were developed using the Support Vector Machines algorithm[22] applied on the PCA projections. Cross-validation and receiver operating characteristic analysis were used to assess the predictors' performance on the data set.

RESULTS

Patient Cohort Characteristics

This retrospective discovery cohort of biobanked and clinically phenotyped patients from Tenon Hospital in Paris included serum from patients with biopsy-proven MCD ($n = 15$) and MN ($n = 37$) collected at the time of biopsy before any immunosuppressive treatment. Serum samples from adult healthy controls ($n = 20$, 13 males, 7 females, mean age 41.2 years) were obtained from the Etablissement Français du Sang in Lyon, France. Figure 1 illustrates the clinical characteristics of the study sample used for the SOMAscan analysis. All patients consented to participate in this study.

SOMAscan Proteomics Identifies a Serum Protein Signature Associated With MCD and MN

SOMAscan analysis of 1305 proteins was performed on the serum samples from 52 adult patients with biopsy-proven MCD ($n = 15$) and MN ($n = 37$) (sex-aggregated) and identified diagnostic serum biomarkers in this

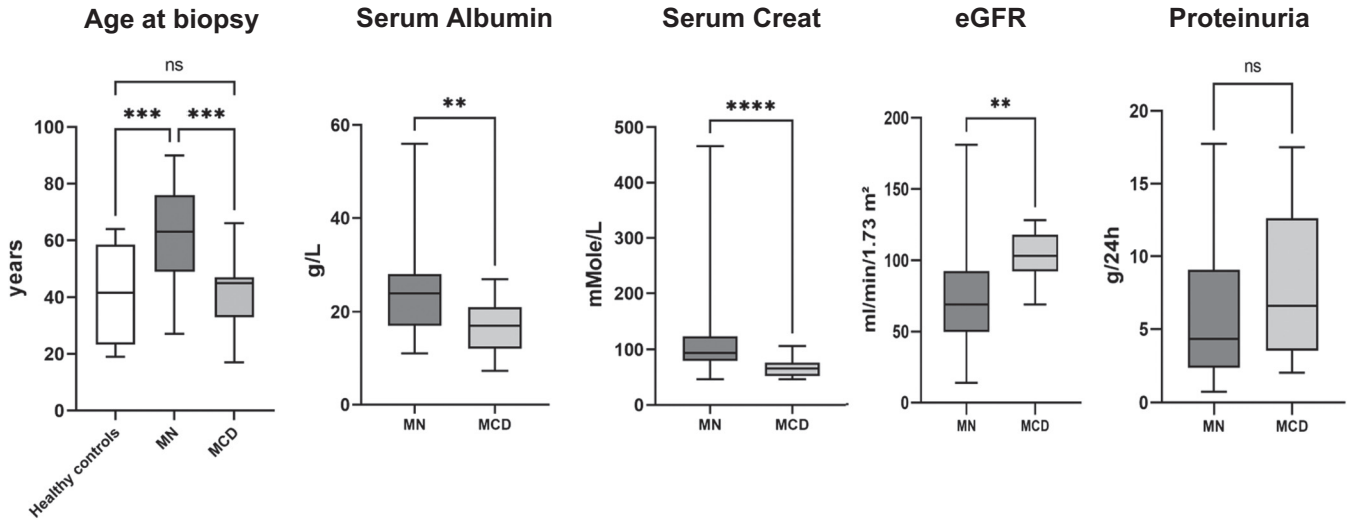

Figure 1. Characteristics of the patients with MN and MCD. Age, serum albumin, serum creatinine, eGFR, and proteinuria of patient cohort. Data are expressed as median and interquartile range. Error bars represent the smallest and the largest values. Differences between patients with MN and MCD were compared by using *t* test when distribution was normal or the Mann-Whitney *U* test for nonparametric distribution. $^{**}P < 0.01$, $^{***}P < 0.001$, $^{****}P < 0.0001$. Sex: healthy control 13 M, 7 F; MN: 29 M, 8 F; MCD: 6 M, 9 F. eGFR, estimated glomerular filtration rate; F, female; M, male; MCD, minimal change disease; MN, membranous nephropathy; ns, not significant.

cohort. The *t* test was applied to the SOMAscan data to identify differentially expressed proteins associated with MCD or MN. Of 1305 measured proteins in the SOMAscan assay panel, 208 proteins were identified that differentiated MCD from healthy controls with high statistical significance (BH-adjusted $P < 0.0001$), whereas 244 proteins differentiated MN from the healthy controls (BH-adjusted $P < 0.0001$) (Supplementary Tables S1 and S2). Importantly, 157 proteins were identified by *t* test to discriminate between MN and MCD with a BH-adjusted $P < 0.05$ consistent with distinct pathophysiological states rather than shared protein dysregulation simply related to the nephrotic syndrome (Supplementary Table S3).

To further define the MN- and MCD-associated proteins in relation to the healthy controls, we performed a pattern analysis on the differentially expressed protein lists. Figure 2a illustrates the 8 most informative patterns of protein expression which were further explored to capture proteins that are uniquely increased or decreased in MN (P1, P2) or MCD (P3, P4) and the proteins that are most often changing compared with the healthy controls (N), either in the same direction (P5, P6) or in opposite direction (P7, P8) (Supplementary Tables S4–S11). There were 406 proteins (P5, P6) that were similarly differentially expressed in MN and MCD compared with the healthy controls (203 increased, 203 decreased; BH $P < 0.05$; Supplementary Tables S8 and S9). In addition, 44 proteins (P1, P2) were exclusively differentially regulated in MN with 20 proteins increasing and 24 decreasing in MN compared with MCD and healthy controls with high significance (BH $P < 0.05$) (Table 1 and Supplementary Tables S4 and S5). A signature of 65 significant differentially expressed proteins (BH $P < 0.05$) was identified, which was exclusively associated with MCD (P3, P4) as compared with MN and healthy controls: 32 proteins were elevated in patients with MCD but 33 proteins were decreased as compared with MN and the controls (Table 2 and Supplementary Tables S6 and S7). Moreover, there were 5 unique proteins (P7, P8) with altered expression in both MN and MCD as compared with healthy controls but in opposite direction (Table 3 and Supplementary Tables S10 and S11). Complete lists of differentially expressed proteins (BH $P < 0.05$) for MN or MCD are available in the Supplementary Data (Supplementary Tables S1–S3).

Hierarchical clustering of the 49 differentially expressed proteins for MN from combining P1, P2, P7, and P8 reveals excellent discrimination between the MN cases and MCD or the healthy controls (Figure 2b, left), with 2 MCD and 2 MN cases misclassified. Similarly, hierarchical clustering of the 70 differentially expressed proteins for MCD from combining P3, P4, P7, and P8 discriminates between the MCD cases and MN or the healthy controls (Figure 2b, right). Applying a second unsupervised learning method, PCA, combined with machine learning, support vector machines, to the 49-protein MN signature also effectively separated the MN cases into distinct clusters from MCD and normal as revealed by the support vector machine classification decision line with a leave-one-out-cross-validation (L1OXV) accuracy of 88.89%

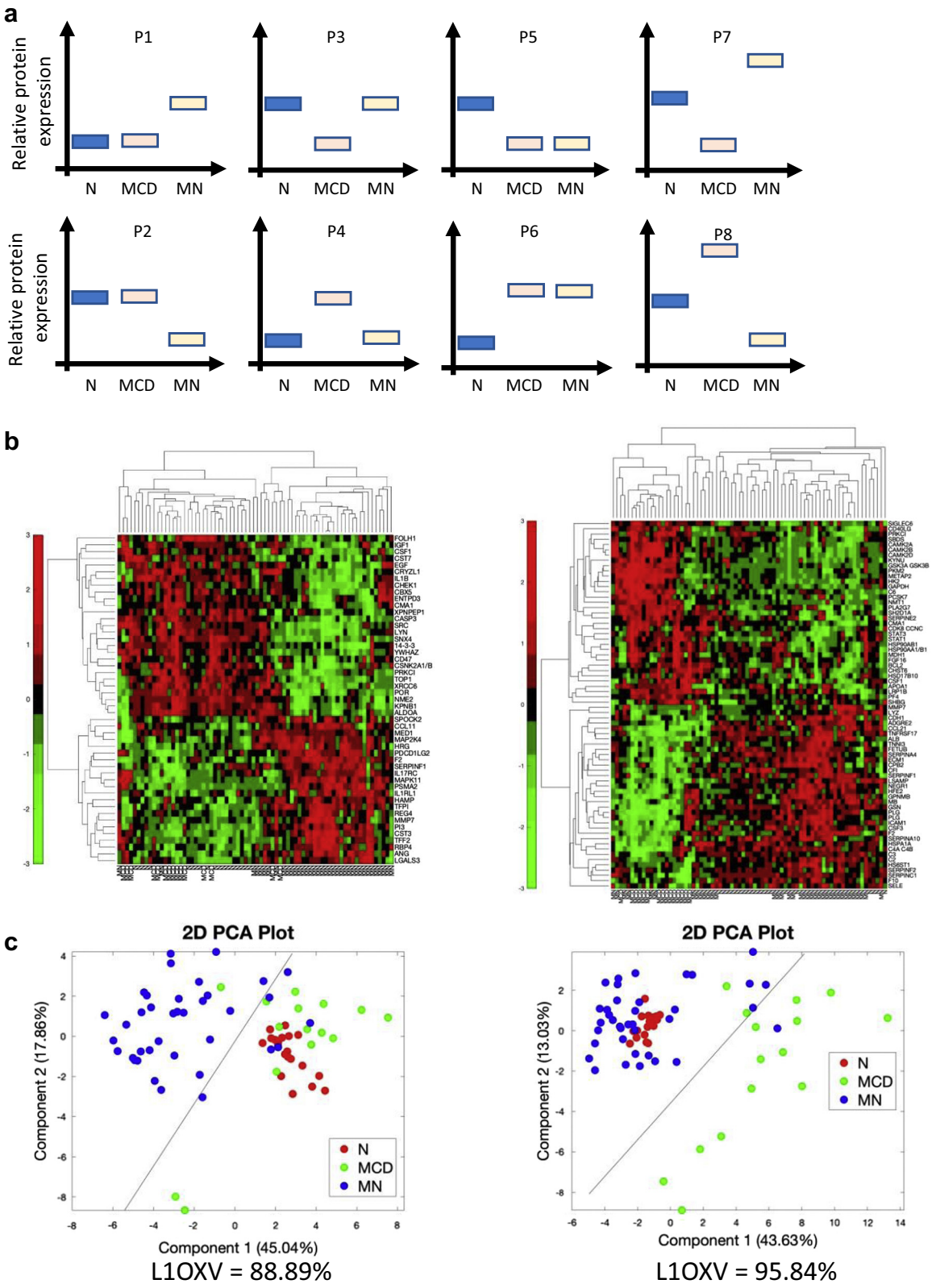

Figure 2. Analysis of protein signatures in patients with MN, patients with MCD, and healthy controls. (a) Protein expression patterns used in pattern analysis. Y-axis represents directional protein expression relative to each patient group. (b) Hierarchical clustering heatmaps of 49 proteins discriminating MN from N and MCD (left) and of 70 proteins discriminating MCD from N and MN (right). (c) PCA using differentially expressed proteins in MN versus N and MCD (L1OXV: 88.89% 49 proteins, BH $P < 0.05$) (left) and MCD versus NM and N (L1OXV: 95.84%, 70 proteins, BH $P < 0.0001$) (right). 2D, 2-dimensional; BH, Benjamin-Hochberg; MCD, minimal change disease; MN, membranous nephropathy; N, healthy controls; PCA, principal component analysis.

Table 2. Differentially regulated proteins in MCD versus MN and N

Gene symbol	Fold change (MCD/N)	BH *P* value	Fold change (MN/N)	BH *P* value	Fold change (MN/MCD)	BH *P* value
Downregulated proteins between MCD vs. MN and N						
SERPINC1	−3.72	0.000002	−1.03	0.338395	3.60	0.000004
MB	−1.82	0.000096	1.15	0.4016	2.10	0.000161
SERPINA4	−1.80	0	−1.12	0.107929	1.60	0.000237
ALB	−2.28	0	1.17	0.985698	2.67	0.000564
GSN	−1.87	0.000001	−1.13	0.070443	1.66	0.001385
ECM1	−2.58	0	1.08	0.607571	2.79	0.001385
LSAMP	−1.39	0.000011	1.03	0.985698	1.42	0.001493
CCL21	−1.81	0.000002	−1.11	0.222296	1.63	0.001734
PLG	−1.36	0.001929	1.16	0.474276	1.58	0.00177
C2	−1.40	0.007913	1.15	0.200447	1.60	0.00177
TNFRSF17	−2.04	0	−1.02	0.387944	2.00	0.00283
F10	−1.64	0.000259	−1.01	0.588567	1.62	0.003873
CSF3	−1.55	0.007887	1.11	0.494808	1.71	0.003908
NEGR1	−1.22	0.000635	1.07	0.478089	1.30	0.006661
C4A C4B	−2.05	0.00016	−1.06	0.286801	1.94	0.007021
CFI	−1.45	0.000243	−1.13	0.09184	1.28	0.0078
LYZ	−1.47	0.001542	1.25	0.393563	1.84	0.009332
HFE2	−1.21	0.007366	1.20	0.116509	1.45	0.009332
PLG	−1.20	0.025261	1.24	0.157171	1.49	0.010427
SELE	−1.32	0.01872	1.11	0.419308	1.47	0.011256
ICAM1	−1.39	0.004763	1.03	0.965462	1.43	0.013733
GPNMB	−1.24	0.020145	1.10	0.414034	1.35	0.014591
HSPA1A	−2.19	0.000004	−1.06	0.221219	2.06	0.015394
ADGRE2	−1.55	0.000086	1.04	0.837462	1.62	0.015574
CPB2	−1.28	0.006093	1.14	0.397549	1.47	0.016852
F2	−1.43	0.037542	1.85	0.062853	2.63	0.018823
SERPINA10	−1.95	0.000122	−1.08	0.353543	1.80	0.019855
CDH1	−1.16	0.041846	1.25	0.078818	1.44	0.020803
SERPINF2	−1.55	0.001612	−1.02	0.448276	1.52	0.021726
TNNI3	−1.10	0.027571	1.03	0.599307	1.13	0.03199
C3	−1.18	0.041614	−1.01	0.736147	1.16	0.038653
FETUB	−1.55	0.000632	−1.06	0.306159	1.46	0.041866
HS6ST1	−1.25	0.026868	1.03	0.974506	1.28	0.042591
Upregulated proteins between MCD vs. MN and N						
SBDS	1.72	0.000498	−1.03	0.395054	−1.78	0.000597
KYNU	1.30	0.000247	−1.02	0.66152	−1.32	0.000843
METAP2	7.83	0.000028	1.71	0.915127	−4.57	0.000894
GSK3A GSK3B	2.94	0.000147	1.20	0.25078	−2.46	0.00168
C6	3.38	0.000058	1.32	0.127974	−2.56	0.002191
LRP1B	1.97	0.000001	1.15	0.778599	−1.72	0.003162
APOA1	3.59	0.005067	−1.15	0.094676	−4.12	0.003485
STAT1	2.37	0.000042	1.26	0.116509	−1.88	0.003629
HSP90AB1	1.31	0.029246	−1.10	0.107385	−1.43	0.006366
CAMK2D	1.95	0.000131	1.13	0.852762	−1.72	0.006661
CDK8 CCNC	1.20	0.002463	−1.02	0.475887	−1.23	0.00668
PF4	1.25	0.000564	−1.02	0.578802	−1.27	0.008201
CD40LG	1.23	0.003407	−1.04	0.369822	−1.28	0.009332
STAT3	1.52	0.002058	1.03	0.990527	−1.47	0.012338
SHBG	2.20	0.010119	1.07	0.391606	−2.07	0.014744
NMT1	1.26	0.045721	−1.05	0.858494	−1.32	0.015001
PKM2	9.28	0.000922	2.02	0.503864	−4.59	0.015574
SIGLEC6	1.33	0.000394	1.09	0.110022	−1.23	0.016068
CHST6	1.23	0.00876	1.02	0.644887	−1.21	0.018056
CAMK2B	1.59	0.000168	1.12	0.503864	−1.42	0.018117
HSP90AA1 HSP90AB1	1.29	0.016884	−1.08	0.204635	−1.40	0.019855
MDH1	1.45	0.038679	−1.07	0.219115	−1.55	0.020476
GAPDH	11.84	0.012164	1.85	0.735882	−6.40	0.023378
CAMK2A	1.24	0.003267	1.00	0.748236	−1.24	0.027486

(Continued on following page)

Table 2. (Continued) Differentially regulated proteins in MCD versus MN and N

Gene symbol	Fold change (MCD/N)	BH *P* value	Fold change (MN/N)	BH *P* value	Fold change (MN/MCD)	BH *P* value
PCSK7	1.25	0.000835	1.02	0.994768	−1.22	0.03089
BCL2	1.29	0.000186	1.07	0.321891	−1.20	0.03199
HK2	1.92	0.007998	1.11	0.556555	−1.72	0.032104
SERPINE2	1.18	0.03496	−1.10	0.19643	−1.29	0.032685
FGF16	1.47	0.001408	1.09	0.501584	−1.35	0.039025
SH2D1A	2.04	0.000147	1.33	0.109965	−1.53	0.039783
PLA2G7	1.43	0.00088	1.08	0.784118	−1.32	0.044187
HSD17B10	1.22	0.012986	1.02	0.884234	−1.20	0.046149

BH, Benjamin-Hochberg; MCD, minimal change disease; MN, membranous nephropathy; N, healthy controls.

(Figure 2c). The 70-protein MCD signature revealed a discrimination from MN and healthy controls by PCA with a L1OXV accuracy of 95.84% (Figure 2c).

Highly discriminatory proteins (Tables 2 and 3, Supplementary Tables S6, S7, S10, and S11) identified in the 70-protein MCD signature included members of the Serpin family (SERPINA10, SERPINA4, SERPINC1, SERPINF2, SERPINF1) that are decreased in MCD compared with MN and healthy controls. Likewise, several members of the complement system (C2, C3, C4A C4B, CFI) and coagulation pathway (F2, F10) are decreased in MCD compared with MN and healthy controls. Most prominently increased in MCD are immune and growth factor signaling proteins, such as STAT1, STAT3, CD40LG, and FGF16, and proteins involved in carbohydrate and lipid metabolism, including GAPDH, GSK3A/B, PKM2, HK2, CHST6, LRP1B, APOE, and APOA1. Most prominently dysregulated in the 49-protein MN signature as compared with MCD and healthy controls were proteins involved in inflammation and cytokine and growth factor signaling, such as IL1RL1, IL17RC prothrombin (F2), CCL11, MAPK11, and MAP2K4, which were increased whereas CASP3, CD47, IGF1, LYN, SRC, IL1B, and EGF were reduced in MN (Tables 1 and 3, Supplementary Tables S4, S5, S10, and S11). As expected, the overall MN phenotype seems generally more inflammatory than MCD. Only a small number of proteins were differentially expressed in MN and MCD when compared with healthy controls but with opposite directionality. MMP7 and SERPINF1 were significantly elevated in MN but reduced in MCD compared with the healthy controls. In contrast, CSF1 was increased in MCD but decreased in MN compared with the healthy controls. Finally, and consistent with dyslipidemia found in the nephrotic syndrome, patients with MCD displayed higher levels of APOA1, APOE (ApoE-2, ApoE3, ApoE-4), PKM2, and FABP1, which play a role in cholesterol transport and long-chain fatty acid metabolism but also have immunoregulatory effects.[23–25] Patients with MN also had increased levels of APOE (ApoE-2, ApoE3, ApoE-4) and FABP1 compared with healthy controls, but to a lesser extent than patients with MCD.

Importantly for differential diagnosis of MCD from MN, a 69-protein signature (BH $P < 0.01$) provided good distinction between MCD and MN by hierarchical clustering and PCA with a L1OXV accuracy of 94.23% (Figure 3a). Thus, SOMAscan effectively defined distinct protein signatures for MN, MCD, and normal healthy controls. To implement the first step for development of a predictor model for discriminating MN from MCD, we evaluated the performance of a support vector machine model with the top 10 discriminatory proteins based on BH *P* value. The L1OXV accuracy of this 10-protein MN/MCD predictor was 92.31% and is visualized by PCA in Figure 3b with an area under the curve of 0.98 (95% CI: 0.95–1.00) in the receiver operating characteristic (Figure 3c).

Functional Annotation and Systems Biology Analysis of Proteins Discriminating MN From MCD and Healthy Controls

In addition to identifying MCD- and MN-segregating biomarkers, SOMAscan analysis provided significant

Table 3. Differentially regulated proteins with opposite directionality in MCD versus MN versus N

Gene symbol	Fold change (MCD/N)	BH *P* value	Fold change (MN/N)	BH *P* value	Fold change (MN/MCD)	BH *P* value
Upregulated in MN; downregulated in MCD						
MMP7	−1.33	0.003381	2.29	0.017799	3.03	0.009332
SERPINF1	−1.52	0.000107	1.23	0.028894	1.87	0.000007
Downregulated in MN; upregulated in MCD						
CSF1	1.36	0.016426	−1.17	0.012089	−1.59	0.00122
CMA1	1.16	0.037685	−1.10	0.04524	−1.28	0.01166
PRKCI	1.18	0.012164	−1.16	0.000934	−1.37	0.000108

BH, Benjamin-Hochberg; MCD, minimal change disease; MN, membranous nephropathy; N, healthy controls.

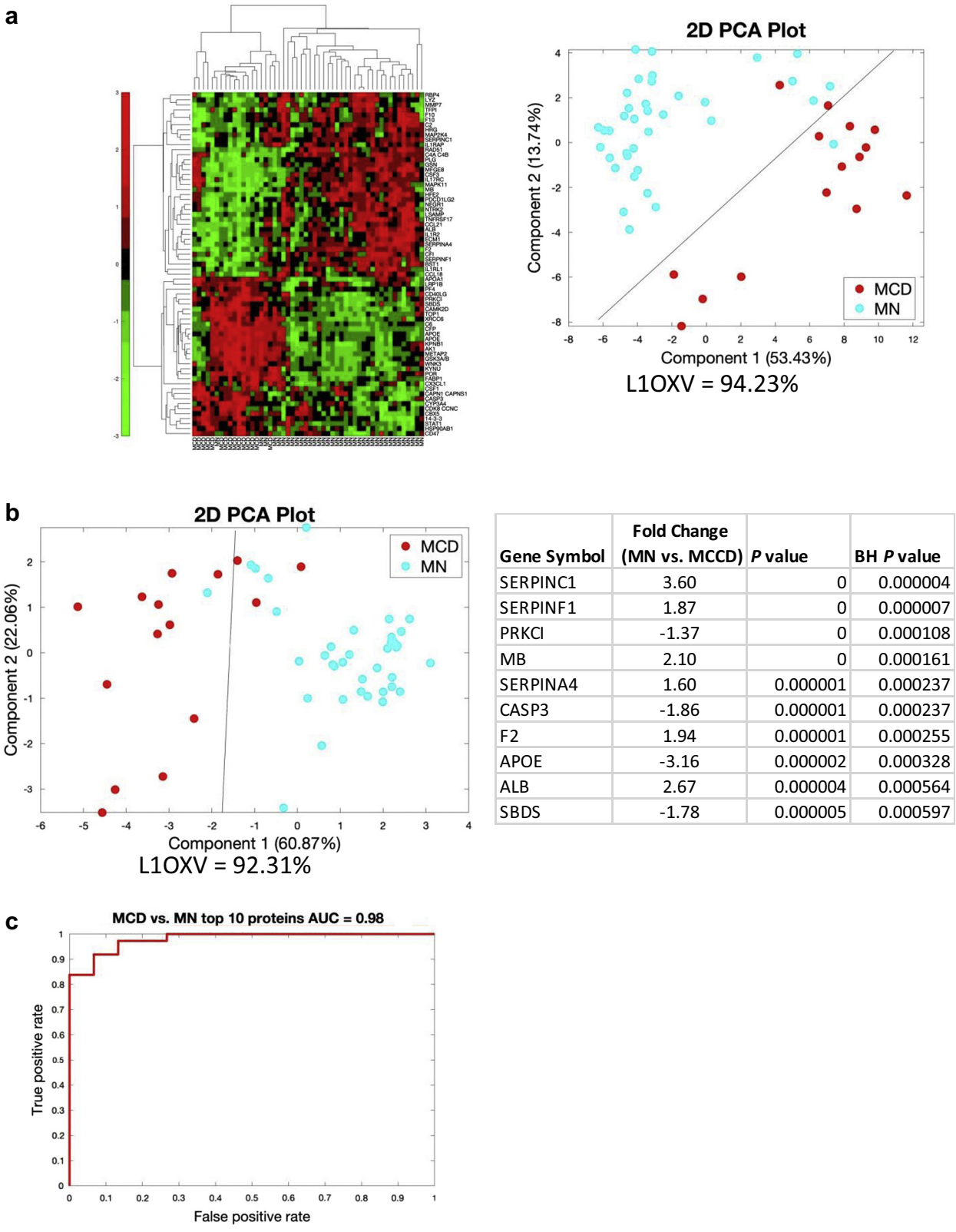

Gene Symbol	Fold Change (MN vs. MCCD)	*P* value	BH *P* value
SERPINC1	3.60	0	0.000004
SERPINF1	1.87	0	0.000007
PRKCI	-1.37	0	0.000108
MB	2.10	0	0.000161
SERPINA4	1.60	0.000001	0.000237
CASP3	-1.86	0.000001	0.000237
F2	1.94	0.000001	0.000255
APOE	-3.16	0.000002	0.000328
ALB	2.67	0.000004	0.000564
SBDS	-1.78	0.000005	0.000597

Figure 3. Analysis of protein signatures comparing patients with MN with those with MCD. (a) Hierarchical clustering heatmap of 69 proteins discriminating MN from N and MCD (left). PCA using differentially expressed proteins in MN versus MCD (L1OXV: 94.23% 69 proteins, BH $P <$ 0.01) (right). (b) PCA and machine learning (SVM) analysis using the top 10 differentially expressed protein between MN and MCD (BH $P < 0.01$ proteins; L1OXV $=$ 92.31%). (c) ROC analysis using the top 10 differentially expressed protein between MN and MCD (BH $P < 0.01$ proteins; AUC $=$ 0.98 [95% CI: 0.95–1.00]). 2D, 2-dimensional; AUC, area under the curve; BH, Benjamin-Hochberg; MCD, minimal change disease; MN, membranous nephropathy; N, healthy controls; PCA, principal component analysis; ROC, receiver operating characteristic; SVM, support-vector machine.

insight into potential disease pathogenesis and pathways enriched in MN or MCD. To identify potential pathophysiological mechanisms that underlie the development of MN pathogenesis and discriminate MN from MCD and healthy controls, and to define the pathways enriched for by the MN-associated proteins, we performed pathway analysis using IPA. For input in IPA, we used the 49 MN-specific proteins (Tables 1 and 3). Particularly informative was the upstream regulator analysis that provides predictions for the most likely proteins affecting expression or activation of downstream target proteins, based on the list of input proteins, with statistical significance and z-scores for prediction of directionality of regulation. This analysis using the IPA database revealed that the statistically most significantly enriched upstream regulators include various cytokines (interleukin [IL]-6, IL-4, TNF, IL-1A, IL-10, IL-3, CCL2), growth factors, hormones, and their receptors (TGFB1, EGFR, KITLG, FGF2, VIP), and transcriptional regulators (CEBPB, SMARCA4) (Figure 4a and Supplementary Table S12). In particular, EGFR was predicted as one of the most significant upstream regulators of 11 of the 49 differentially regulated proteins in patients with MN as compared with patients with MCD and healthy controls (Figure 4a and b). Of 49 proteins, 13 are predicted to be regulated by the proinflammatory cytokines IL-6 or IL-4 in patients with MN as compared with patients with MCD and healthy controls, and of the 49 MN proteins, 17 are downstream of TGFB1 (Figure 4a and b).

When applying IPA for determining the significantly enriched disease and biological functions, we identified as most prominent with the highest statistical significance a predicted enhancement of cell survival pathways (cell survival, apoptosis, cell viability, necrosis, cell death of immune cells, necrosis of epithelial tissue, cell death of epithelial cells) (Figure 4c and d and Supplementary Table S13). Apoptosis and necrosis were predicted to be increased based on the activation z-score being around or above 2.0 and included statistically significant enhanced cell death of kidney cells, apoptosis of kidney cell lines, and decreased proliferation of kidney cells and growth of the glomerulus (Figure 4c and d). Of 49 proteins, 35 were directly linked to apoptosis, necrosis, cell death of immune cells, cell survival, and cell viability. A subset of 10 proteins was associated with increased apoptosis of kidney cell lines and cell death of kidney cells and decreased proliferation of kidney cells and glomerular cells (Figure 4d) suggesting patients with MN may exhibit increased cell death in comparison to patients with MCD and healthy controls.

Additional biofunctions significantly enriched in MN-specific serum proteins involved immune and inflammatory functions (inflammatory response, activation of antigen-presenting cells, activation of phagocytes, stimulation of leukocytes, inflammation of organ, activation of myeloid cells, inflammation of absolute anatomic region, leukopoiesis, activation of macrophages, immune response of leukocytes, inflammation of body cavity), fatty acid metabolism (synthesis of eicosanoid, fatty acid metabolism, synthesis of lipid, synthesis of prostaglandin), vascular function (development of vasculature, vasculogenesis, angiogenesis, neovascularization), and synthesis and generation of reactive oxygen species (Figure 4d).

Functional Annotation and Systems Biology Analysis of Proteins Discriminating MCD From MN and Healthy Controls

Upstream regulator analysis of the 70 proteins associated specifically with MCD was dominated by TGFB1, MYC, and LPL that are predicted to be activated in MCD and KDM6A that is predicted to have decreased activity in MCD with activation z-scores >2.0 (Figure 5a and b and Supplementary Table S14). The statistically most significant upstream regulators also included several cytokines (IL-1, IL-6, IFNG, TNF, IL-15, IL-2), transcription factors (TP53, NFKBIA, TP73, PPARG, HIF1A, CEBPA, NFAT, STAT3, EGR1), and miR-155, OSM, IKBKB, COL18A1, KRAS, and APP. Of the 70 proteins, 24 were downstream of TGFB1, indicating the TGFB1 pathway may play an important role in MCD (Figure 5b). Disruption of fatty acid metabolism is a well-known feature of MCD and the nephrotic syndrome. Because decreased LPL activity is associated with impaired lipid clearance, the predicted decrease in LPL activity upstream of 5 MCD proteins explains some of the biochemical changes observed in the nephrotic syndrome (Figure 5b).

Among the disease and biological functions enriched for by the MCD-specific proteins, cell survival functions were statistically highly significant (necrosis, cell viability, cell death of immune cells, cell death of antigen-presenting cells, apoptosis, cell death of phagocytes) with enrichment of 48 of 70 MCD proteins (Figure 5c and d). However, in contrast to the increased cell death predicted in MN, cell death is predicted to be reduced in MCD. Similarly, vascular function (vasculogenesis, angiogenesis, vascularization of absolute anatomic region, vascularization, proliferation of endothelial cells) was significantly enriched and predicted to be enhanced in MCD as compared with the predicted decrease in MN (Figure 5c and Supplementary Table S15). Of 70 MCD proteins, 33 were predicted to be linked to angiogenesis and vasculogenesis (Figure 5d). Decreased movement of immune cells (leukocyte migration, cell movement of

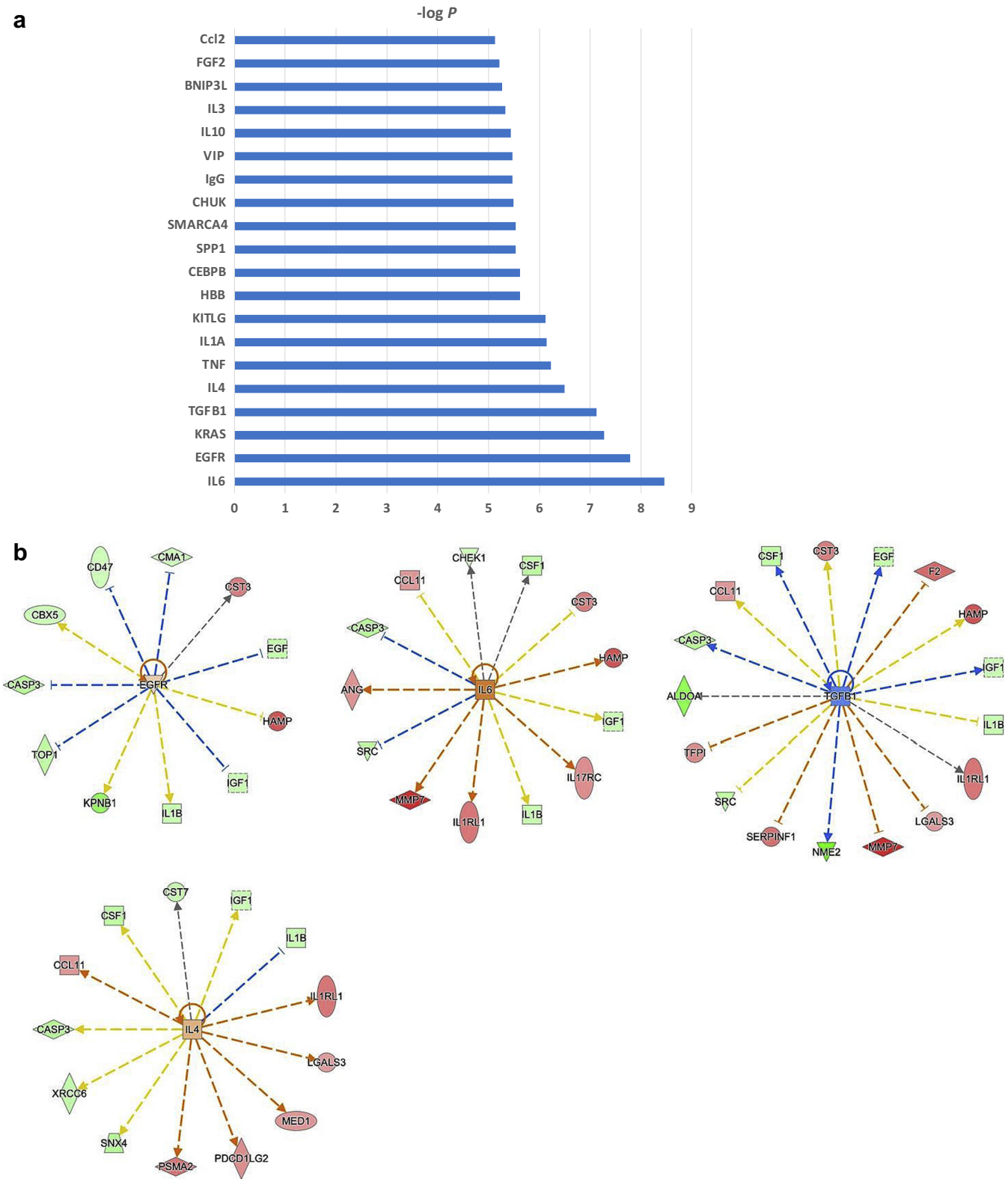

Figure 4. Systems biology analysis in MN. IPA of the 49 significant differentially expressed MN-associated proteins was conducted to identify key upstream regulators (a,b) and biological function associations (c,d) enriched in patients with MN. (a) List of the most significant upstream regulators that best explain the observed expression changes in MN versus N and MCD. (b) A total of 4 significant upstream regulators (EGFR, IL-6, TGFB1, IL-4) and the MN-associated proteins predicted to be downstream of these upstream regulators. IPA color and symbol guide: blue, inhibition; orange, activation; red, increased; green, decreased; yellow, contrary to published evidence; gray, unknown; dashed line, indirect; arrowhead (pointed), activating; arrowhead (blunt), inhibitory. (Continued)

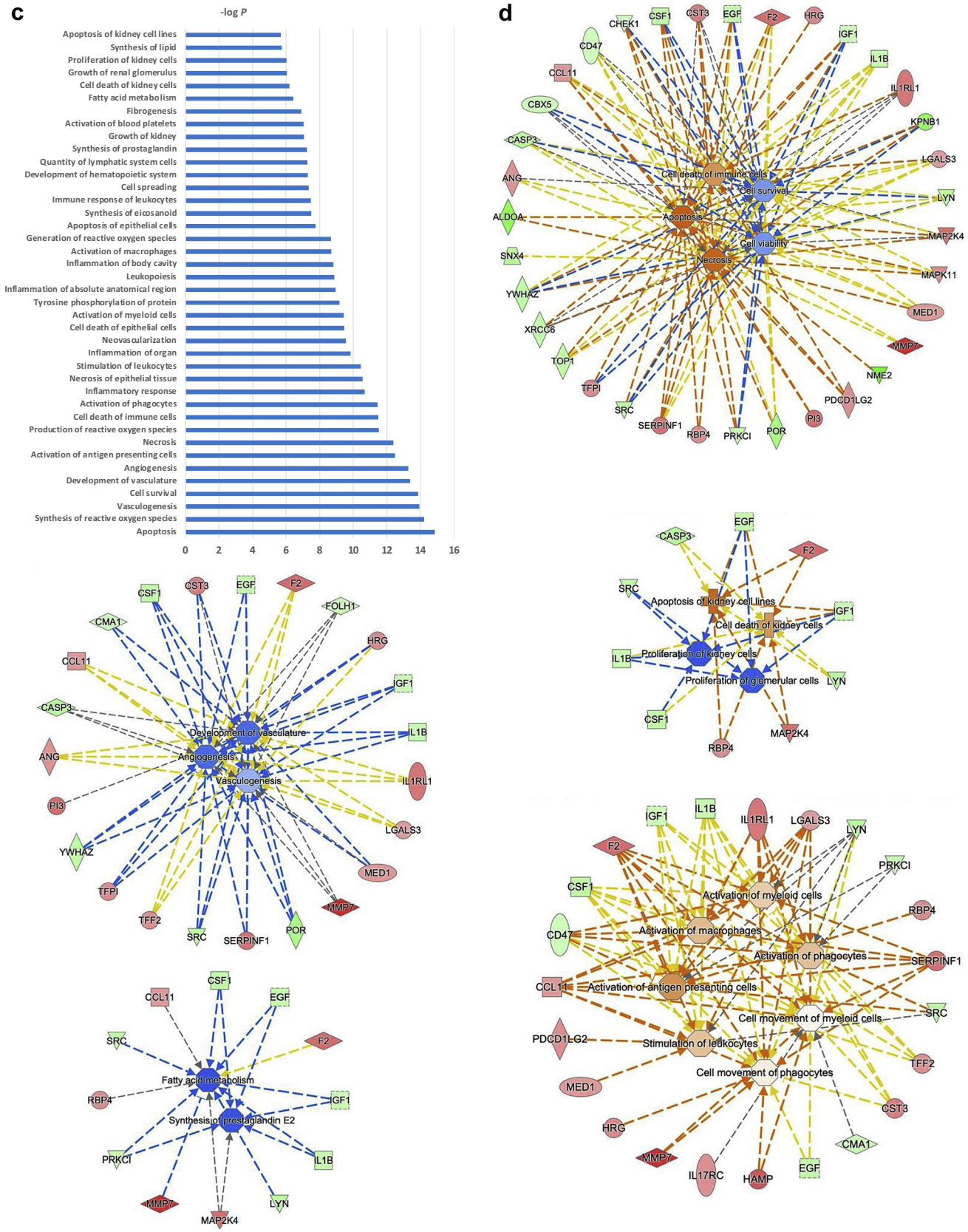

Figure 4. (Continued) (c) List of the most significant biological functions that best explain the observed expression changes in MN versus N and MCD. (d). A total of 5 significant classes of biological functions enriched among the MN-associated 49-protein signature. IL, interleukin; IPA, Ingenuity Pathway Analysis; MCD, minimal change disease; MN, membranous nephropathy; N, healthy controls.

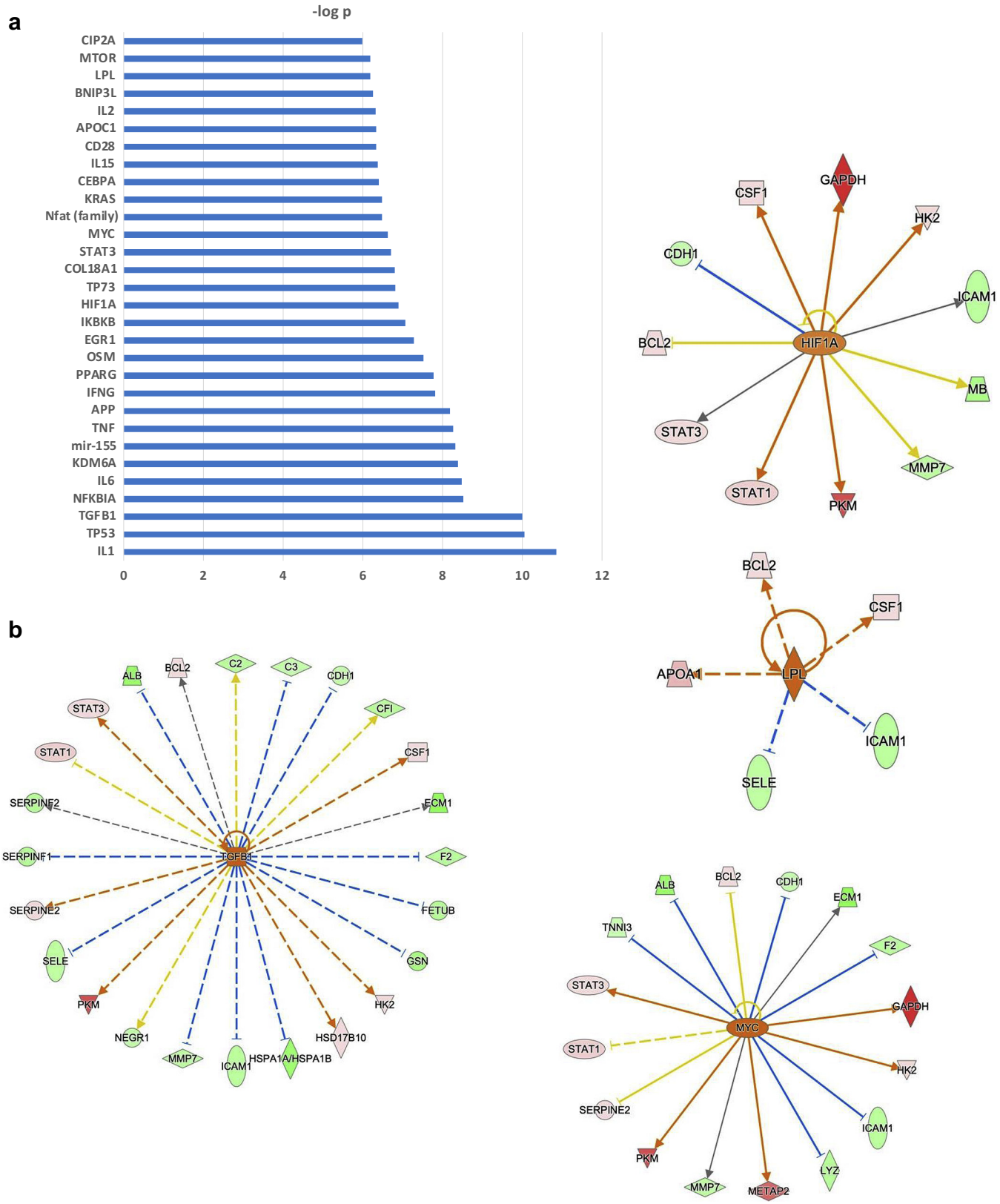

Figure 5. Systems biology analysis in MCD. IPA of the 70 significant differentially expressed MCD-associated proteins was conducted to identify key upstream regulators (a,b) and biological function associations (c,d) enriched in patients with MN. (a) List of the most significant upstream regulators that best explain the observed expression changes in MCD versus N and MN. (b) A total of 4 significant upstream regulators (HIF1A, TGFB1, LPL, MYC) and the MCD-associated proteins predicted to be downstream of these upstream regulators. IPA color and symbol guide: blue, inhibition; orange, activation; red, increased; green, decreased; yellow, contrary to published evidence; gray, unknown; dashed line, indirect; arrowhead (pointed), activating; arrowhead (blunt), inhibitory. (Continued)

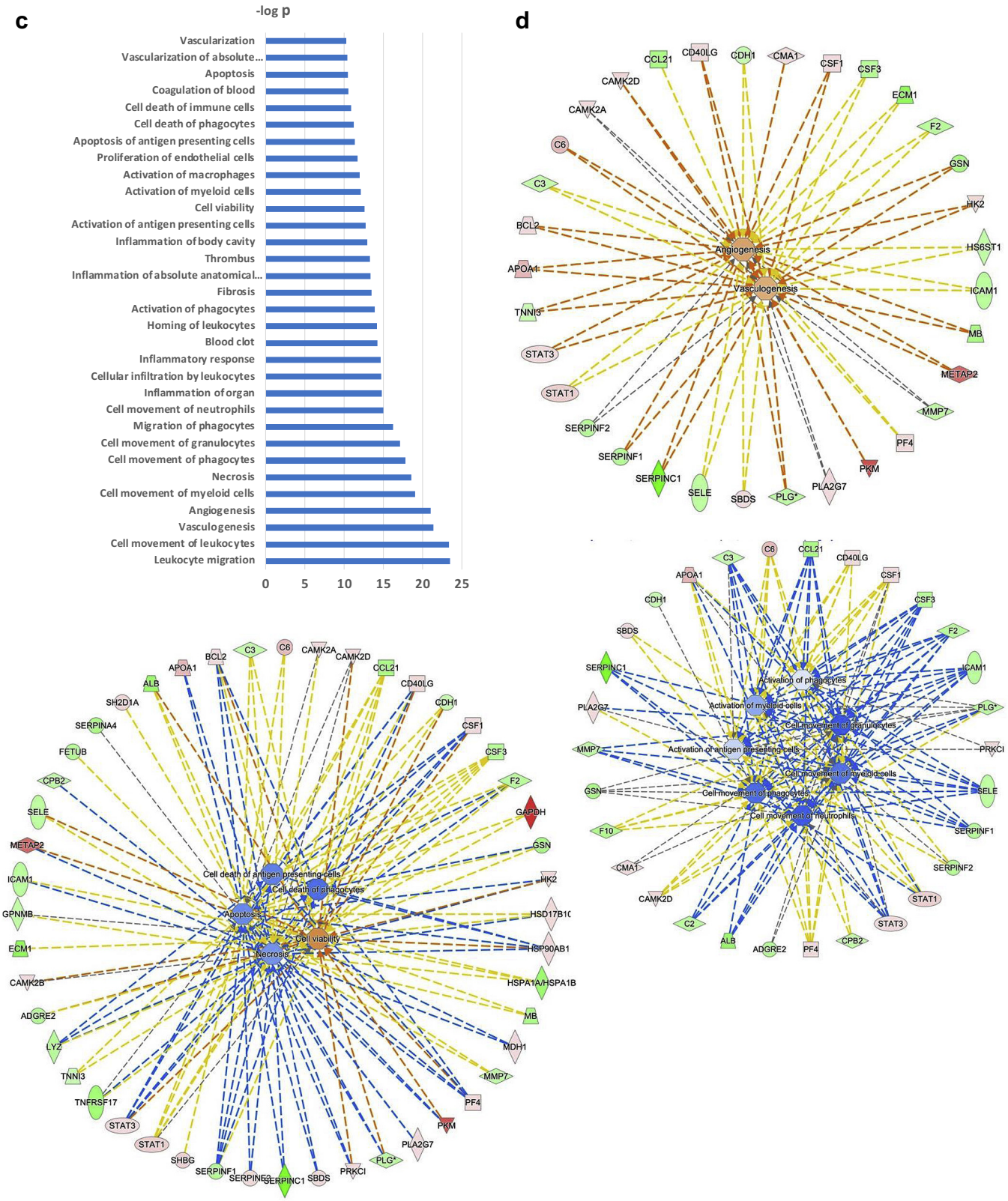

Figure 5. (Continued) (c) List of the most significant biological functions that best explain the observed expression changes in MCD versus N and MN. (d). A total of 3 significant classes of biological functions enriched among the MCD-associated 70-protein signature. IPA, Ingenuity Pathway Analysis; MCD, minimal change disease; MN, membranous nephropathy; N, healthy controls.

leukocytes, cell movement of phagocytes, cell movement of myeloid cells, cell movement of granulocytes, cell movement of neutrophils, cellular infiltration by leukocytes, migration of phagocytes, homing of leukocytes) and activation of immune cells (activation of phagocytes, activation of antigen-presenting cells,

activation of myeloid cells, activation of macrophages) were other highly significant biological functions in MCD (Figure 5c and d). In addition, statistically highly significant were fibrosis, coagulation (blood clot, thrombus, hematologic coagulation of blood), and inflammation (inflammatory response, inflammation of body cavity, inflammation of organ, inflammation of absolute anatomic region) (Figure 5c and d).

DISCUSSION

Applying the novel SOMAscan proteomics platform that measures 1305 proteins across the entire dynamic range of proteins in serum has successfully identified unique serum protein signatures that are consistent with distinct molecular pathways that underlie MCD and MN. Analysis of the pathophysiological pathways associated with the MCD and MN protein signatures indicated that proteins regulating cell death, vascular functions, and inflammatory processes are especially over-represented in the peripheral blood in both patients with MCD and those with MN but primarily in opposite direction. With ongoing refinement and validation, a diagnostic model of multiple new blood biomarkers to existing serologic assays and clinical parameters is anticipated to address fundamental clinical questions and guide key decision points in nephrology practice.

The application of proteomics to MCD and MN has been previously performed primarily in urine and kidney biopsy samples.[26–29] In fact, gel electrophoresis with or without mass spectrometry techniques applied to glomerular protein lysates were primarily used to identify the existing MN antigens, including phospholipase A2 receptor, thrombospondin type 1 domain-containing 7A, bovine serum albumin, and neutral endopeptidase. More recently, a technological leap based on a combination of laser microdissection of the glomeruli and mass spectrometry of the digested extracted proteins led to identification of a series of new "antigens."[26–29] Newer techniques, such as matrix-assisted laser desorption/ionization mass spectrometric imaging, are also being applied for biomarker discovery with promising results in kidney biopsies of patients with MN.[28] The bulk of proteomic work, however, has been performed using conventional mass spectrometry techniques, such as liquid chromatography with tandem mass spectrometry, in the urines of patients with the nephrotic syndrome. Interestingly, we confirm in this study the identification of several biomarkers previously validated in these discovery studies, including C9, SERPINA1, and apolipoprotein-A1, in patients with MCD.[26,29]

Currently, there are no specific and sensitive noninvasive biomarkers for differential diagnosis of MCD or PLA2R-negative MN. Furthermore, the molecular mechanisms underlying MCD and MN etiopathology are not well understood. These questions can be addressed with the SOMAscan proteomics platform. Systems biology analysis of our SOMAscan data revealed, not surprisingly, dysregulation of unique sets of proteins and distinct molecular profiles between MCD and MN, which are independent of the nephrotic syndrome state itself. For example, compared with MCD, MN was associated with increased inflammatory biomarkers, such as IL1RL1 and IL17RC, and dysregulation of many proteins in the complement pathway (C2, C3, C4A/B), consistent with the current experimental and pathologic understanding of podocyte injury in MN.[2] MN was also associated with greater alterations in proteins of the coagulation pathway compared with MCD, including SERPINC1 (antithrombin III), SERPINA10, SERPINF2, F2 (prothrombin), and F10 (factor X), again consistent with the increased risk of thrombotic events in patients with MN.[30] Increased apoptosis in MN was another hallmark observed in our protein signature data and is consistent with glomerular injury that results in cell death and loss of podocytes.[31,32] In contrast, MCD generally displayed a different immune profile and reduced cell death but enhanced vascular functions compared with MN. For example, several proteins involved in adaptive immunity were dysregulated in MCD, including CD40LG, CSF1, TNFRSF17, CCL21, and STAT1/3, in keeping with the proposed disease pathogenesis that involves T and B lymphocytes.[33] Proteins including ICAM-1 and CSF3 that regulate innate cells, such as granulocytes, were decreased in MCD. MCD also displayed protein changes that promote glomerular health and cellular survival. In addition to higher levels of the antiapoptosis proteins BCL2 and PRKCI, patients with MCD had lower levels of the angiogenesis inhibitor, SERPINF1, and increased CMA1 compared with MN. Overall, although these results are hypothesis generating, more basic research is required to fully understand the mechanisms underlying the blood protein changes in MCD and MN and the potential causal relationships in the pathophysiology of MN and MCD.

One of the major obstacles in applying MS-based proteomics to urine samples or biopsy specimens is high-abundance proteins that mask lower abundance, highly disease-relevant proteins. The SOMAscan proteomics assay overcomes this challenge and greatly facilitates discovery proteomics in complex biological samples, such as serum or plasma, that have a dynamic range of protein concentrations exceeding 12 logs. The ability to apply proteomics to serum (or plasma), which are consistent biological fluids, enables reproducibility more so than the variability inherent in urine or tissue

biopsies. Our study represents the first application of SOMAscan proteomics for nephrotic syndrome and provides a data set for further investigation and validation. The major drawback with SOMAscan, however, is the limited number of analytes available in the assay used for the current study (approximately 1300) which, consequently, misses proteins more specific for function in the kidney. This number has increased as the technology matures, and assays are now available that can measure 7000 proteins. Our results and pathway analyses reported here cannot aid in distinguishing proteins dysregulated as a primary, causal pathogenic process versus those that change as part of the adaptive response to pathology. Nevertheless, longitudinal studies could lead to better understanding of the relevance of some of these proteins as drivers of disease pathogenesis.

This was an exploratory study of the aptamer-based SOMAscan platform in a discovery cohort of patients with MN and MCD. Our study is limited by the small sample size. Yet, it provides important new information and insights to better understand the similarities and differences between MN and MCD. In contrast to identifying differential expression of a small number of dominant proteins that could be developed as single disease biomarkers, the data uncovered significant dysregulation of protein signatures linked to biological pathways in MN and MCD. The biomarker signatures revealed by the SOMAscan assay were able to differentiate MCD from MN with high statistical accuracy and an area under the curve of 0.98 (95% CI: 0.95–1.00). Although our data are promising, the reproducibility and clinical accuracy of these discovery biomarker signatures require independent, prospective validation in larger, well-phenotyped patient cohorts, and comparison to healthy controls and other GNs, such as primary focal segmental glomerulosclerosis, before refinement and validation using more clinically useful multiplex immunoassays. In this regard, SOMAscan analysis would first be performed on an independent test set of samples, followed by a prospective, larger scale cohort if the predictor performance on the independent test set is close to the one observed on the training set. Ultimately, a new and improved diagnostic paradigm that uses a combination of these protein signatures/biomarkers, anti-PLA2R or anti-THSD7A serologic tests, in conjunction with clinical parameters may improve the differential diagnosis of MN and MCD and provide better stratification and management of patients with nephrotic syndromes.

DISCLOSURE

All the authors declared no competing interests.

ACKNOWLEDGMENTS

The authors thank the clinicians who took care of the patients and all staff members of the Tenon Hospital Biological Resource Center (BRC CANCER Hôpitaux Universitaires de l'Est Parisien-Paris) for their help in centralizing and managing biological data collection. This study and the biorepository of the Tenon Hospital Biological Resource Center were funded by grants from the European Research Council ERC-2012-ADG_20120314 (Grant Agreement 322947) and from the Seventh Framework Programme of the European Community Contract 2012–305608 (European Consortium for High-Throughput Research in Rare Kidney Diseases). Research funding was also provided by the Department of Medicine at the University of Calgary. PR is a recipient of the National Research Agency grants Membranous Nephropathy Aims (ANR-17-CE17-0012-01) and SeroNegative Membranous Nephropathy (ANR-20-CE17-0017-01).

SUPPLEMENTARY MATERIAL

Supplementary Tables S1–S3 (Excel)

Table S1. Differentially expressed proteins in minimal change disease versus healthy controls.

Table S2. Differentially expressed proteins in membranous nephropathy versus healthy controls.

Table S3. Differentially expressed proteins in membranous nephropathy versus minimal change disease.

Supplementary Tables S4–S11 (Excel)

Table S4. Upregulated proteins in membranous nephropathy versus minimal change disease and healthy controls.

Table S5. Downregulated proteins in membranous nephropathy versus minimal change disease and healthy controls.

Table S6. Downregulated proteins in minimal change disease versus membranous nephropathy and healthy controls.

Table S7. Upregulated proteins in minimal change disease versus membranous nephropathy and healthy controls.

Table S8. Downregulated proteins in minimal change disease and membranous nephropathy versus healthy controls.

Table S9. Upregulated proteins in minimal change disease and membranous nephropathy versus healthy controls.

Table S10. Differentially expressed proteins upregulated in membranous nephropathy and downregulated in minimal change disease versus healthy controls.

Table S11. Differentially expressed proteins downregulated in membranous nephropathy and upregulated in minimal change disease versus healthy controls.

Supplementary Tables S12–S15 (Excel)

Table S12. Upstream regulators for P1 P2 P7 P8. Membranous nephropathy versus minimal change disease and healthy controls.

Table S13. Biological functions for P1 P2 P7 P8. Membranous nephropathy versus minimal change disease and healthy controls.

Table S14. Upstream regulators for P3 P4 P7 P8. Minimal change disease versus membranous nephropathy and healthy controls.

Table S15. Biological functions for P3 P4 P7 P8. Minimal change disease versus membranous nephropathy and healthy controls.

REFERENCES

1. McGrogan A, Franssen CF, de Vries CS. The incidence of primary glomerulonephritis worldwide: a systematic review of the literature. *Nephrol Dial Transplant*. 2011;26:414–430. https://doi.org/10.1093/ndt/gfq665
2. Ronco P, Debiec H. Pathophysiological advances in membranous nephropathy: time for a shift in patient's care. *Lancet*. 2015;385:1983–1992. https://doi.org/10.1016/S0140-6736(15)60731-0
3. McMahon GM, McGovern ME, Bijol V, et al. Development of an outpatient native kidney biopsy service in low-risk patients: a multidisciplinary approach. *Am J Nephrol*. 2012;35:321–326. https://doi.org/10.1159/000337359
4. Samuel SM, Takano T, Scott S, et al. Setting new directions for research in childhood nephrotic syndrome: results from a national workshop. *Can J Kidney Health Dis*. 2017;4:2054358117703386. https://doi.org/10.1177/2054358117703386
5. Pourcine F, Dahan K, Mihout F, et al. Prognostic value of PLA2R autoimmunity detected by measurement of anti-PLA2R antibodies combined with detection of PLA2R antigen in membranous nephropathy: a single-centre study over 14 years. *PLoS One*. 2017;12:e0173201. https://doi.org/10.1371/journal.pone.0173201
6. Cattran DC, Brenchley PE. Membranous nephropathy: integrating basic science into improved clinical management. *Kidney Int*. 2017;91:566–574. https://doi.org/10.1016/j.kint.2016.09.048
7. De Vriese AS, Glassock RJ, Nath KA, Sethi S, Fervenza FC. A proposal for a serology-based approach to membranous nephropathy. *J Am Soc Nephrol*. 2017;28:421–430. https://doi.org/10.1681/ASN.2016070776
8. Gold L, Walker JJ, Wilcox SK, Williams S. Advances in human proteomics at high scale with the SOMAscan proteomics platform. *N Biotechnol*. 2012;29:543–549. https://doi.org/10.1016/j.nbt.2011.11.016
9. Ganz P, Heidecker B, Hveem K, et al. Development and validation of a protein-based risk score for cardiovascular outcomes among patients with stable coronary heart disease. *JAMA*. 2016;315:2532–2541. https://doi.org/10.1001/jama.2016.5951
10. Daniels JR, Ma JZ, Cao Z, et al. Discovery of novel proteomic biomarkers for the prediction of kidney recovery from dialysis-dependent AKI patients. *Kidney360*. 2021;2:1716–1727. https://doi.org/10.34067/kid.0002642021
11. Gordin D, Shah H, Shinjo T, et al. Characterization of glycolytic enzymes and pyruvate kinase M2 in type 1 and 2 diabetic nephropathy. *Diabetes Care*. 2019;42:1263–1273. https://doi.org/10.2337/dc18-2585
12. Liu RX, Thiessen-Philbrook HR, Vasan RS, et al. Comparison of proteomic methods in evaluating biomarker-AKI associations in cardiac surgery patients. *Transl Res*. 2021;238:49–62. https://doi.org/10.1016/j.trsl.2021.07.005
13. Gold L, Ayers D, Bertino J, et al. Aptamer-based multiplexed proteomic technology for biomarker discovery. *PLoS One*. 2010;5:e15004. https://doi.org/10.1371/journal.pone.0015004
14. Lollo B, Steele F, Gold L. Beyond antibodies: new affinity reagents to unlock the proteome. *Proteomics*. 2014;14:638–644. https://doi.org/10.1002/pmic.201300187
15. Mehan MR, Ayers D, Thirstrup D, et al. Protein signature of lung cancer tissues. *PLoS One*. 2012;7:e35157. https://doi.org/10.1371/journal.pone.0035157
16. Shubin AV, Kollar B, Dillon ST, Pomahac B, Libermann TA, Riella LV. Blood proteome profiling using aptamer-based technology for rejection biomarker discovery in transplantation. *Sci Data*. 2019;6:314. https://doi.org/10.1038/s41597-019-0324-y
17. Vasunilashorn SM, Dillon ST, Chan NY, et al. Proteome-wide analysis using SOMAscan identifies and validates chitinase-3-like protein 1 as a risk and disease marker of delirium among older adults undergoing major elective surgery. *J Gerontol A Biol Sci Med Sci*. 2022;77:482–491. https://doi.org/10.1093/gerona/glaa326
18. Benjamini Y, Hochberg Y. Controlling the false discovery rate: a practical and powerful approach to multiple testing. *J Roy Stat Soc B*. 1995;57:289–300.
19. Smyth GK. Linear models and empirical Bayes methods for assessing differential expression in microarray experiments. *Stat Appl Genet Mol Biol*. 2004;3:3. https://doi.org/10.2202/1544-6115.1027
20. Otu HH, Naxerova K, Ho K, et al. Restoration of liver mass after injury requires proliferative and not embryonic transcriptional patterns. *J Biol Chem*. 2007;282:11197–11204. https://doi.org/10.1074/jbc.M608441200
21. Krämer A, Green J, Pollard J Jr, Tugendreich S. Causal analysis approaches in Ingenuity Pathway Analysis. *Bioinformatics*. 2014;30:523–530. https://doi.org/10.1093/bioinformatics/btt703
22. Hsu CW, Lin CJ. A comparison of methods for multiclass support vector machines. *IEEE Trans Neural Netw*. 2002;13:415–425. https://doi.org/10.1109/72.991427
23. Kanaguchi Y, Suzuki Y, Osaki K, Sugaya T, Horikoshi S, Tomino Y. Protective effects of L-type fatty acid-binding protein (L-FABP) in proximal tubular cells against glomerular injury in anti-GBM antibody-mediated glomerulonephritis. *Nephrol Dial Transplant*. 2011;26:3465–3473. https://doi.org/10.1093/ndt/gfr110
24. Li Y, Dong JB, Wu MP. Human ApoA-I overexpression diminishes LPS-induced systemic inflammation and multiple organ damage in mice. *Eur J Pharmacol*. 2008;590:417–422. https://doi.org/10.1016/j.ejphar.2008.06.047
25. Vitek MP, Brown CM, Colton CA. APOE genotype-specific differences in the innate immune response. *Neurobiol Aging*. 2009;30:1350–1360. https://doi.org/10.1016/j.neurobiolaging.2007.11.014
26. Choi YW, Kim YG, Song MY, et al. Potential urine proteomics biomarkers for primary nephrotic syndrome. *Clin Proteomics*. 2017;14:18. https://doi.org/10.1186/s12014-017-9153-1
27. Perez V, Lopez D, Boixadera E, et al. Comparative differential proteomic analysis of minimal change disease and focal

segmental glomerulosclerosis. *BMC Nephrol*. 2017;18:49. https://doi.org/10.1186/s12882-017-0452-6

28. Smith A, L'Imperio V, Ajello E, et al. The putative role of MALDI-MSI in the study of Membranous Nephropathy. *Biochim Biophys Acta*. 2017;1865:865–874. https://doi.org/10.1016/j.bbapap.2016.11.013
29. Suresh CP, Saha A, Kaur M, et al. Differentially expressed urinary biomarkers in children with idiopathic nephrotic syndrome. *Clin Exp Nephrol*. 2016;20:273–283. https://doi.org/10.1007/s10157-015-1162-7
30. Huang MJ, Wei RB, Wang ZC, et al. Mechanisms of hypercoagulability in nephrotic syndrome associated with membranous nephropathy as assessed by thromboelastography. *Thromb Res*. 2015;136:663–668. https://doi.org/10.1016/j.thromres.2015.06.031
31. Li J, Chen Y, Shen L, Deng Y. Improvement of membranous nephropathy by inhibition of miR-193a to affect podocytosis via targeting WT1. *J Cell Biochem*. 2019;120:3438–3446. https://doi.org/10.1002/jcb.27616
32. Sun Z, Xu Q, Ma Y, et al. Circ_0000524/miR-500a-5p/CXCL16 axis promotes podocyte apoptosis in membranous nephropathy. *Eur J Clin Investig*. 2021;51:e13414. https://doi.org/10.1111/eci.13414
33. Vivarelli M, Massella L, Ruggiero B, Emma F. Minimal change disease. *Clin J Am Soc Nephrol*. 2017;12:332–345. https://doi.org/10.2215/CJN.05000516